The paper was published in the proceedings of the 10th International Conference on Physical Modelling in Geotechnics and was edited by Moonkyung Chung, Sung-Ryul Kim, Nam-Ryong Kim, Tae-Hyuk Kwon, Heon-Joon Park, Seong-Bae Jo and Jae-Hyun Kim. The conference was held in Daejeon, South Korea from September 19th to September 23rd 2022.

Physical Modelling in Geotechnics

Effect of rainfall intensity on the deformation behaviour of geogrid reinforced soil wall with low-permeable backfill: Centrifuge study

M. Jayanandan & B.V.S. Viswanadham
Department of Civil Engineering, Indian Institute of Technology Bombay, Powai, Mumbai, India

ABSTRACT: The objective of this paper is to comprehensively investigate the effect of rainfall intensity on the performance of a geogrid reinforced soil wall by simulating in-flight rainfall in centrifuge. Two centrifuge model tests were performed on a typical geogrid reinforced soil wall with low-permeable backfill at 40 gravities using a 4.5 m radius large beam geotechnical centrifuge facility available at IIT Bombay, India. The model wall of height 10 m with a 6° inclination with vertical was subjected to rainfall intensities of 10 mm/h and 20 mm/h with the help of specially designed pneumatic nozzles-based rainfall simulator. The analysis and interpretation of centrifuge model tests indicated that with the ingression of rainwater, there was a decline in matric suction, resulting in the rise of phreatic surface and a subsequent increase in positive pore water pressures. The infiltration rate was observed to be faster when the model wall was subjected to higher rainfall intensity, and it experienced a global stability failure in a shorter duration as compared to the model wall subjected to lower rainfall intensity. However, it was observed that the model wall subjected to higher rainfall intensity developed fewer positive pore water pressures. This indicates that when a low-permeable backfill is subjected to rainfall intensity greater than its saturated hydraulic conductivity, the large magnitude of face deformations and surface settlements caused by the subsurface flow contribute to and expedite the failure of the structure, in addition to the instability caused by the loss of matric suction within the soil mass.

Keywords: Geogrid reinforced soil wall, Low-permeable backfill, Rainfall, Pore water pressures, Centrifuge modelling.

1 INTRODUCTION

Geosynthetic reinforced soil walls (GRSW) with low permeable backfill soils are susceptible to rainfall-triggered failures with the instability arising due to the inefficiency of such poorly draining soils (good quality backfill soils with less than 15% fines content passing 0.075 mm sieve and with plasticity index ≤ 6 is mandated by AASHTO (2009)) to dissipate the generated excess pore water pressure. According to Xue and Gavin (2008), at the start of rainfall, infiltration equals rainfall intensity and consequently no runoff occurs. With increasing rainfall intensity, the run-off starts earlier subsequently reducing the infiltration and the run-off continues even after rainfall stops, indicating subsurface (lateral) flow. Yoo et. al. (2021) suggested that for a given total rainfall, the longer but lower intensity rainfall induced facing displacements of similar magnitudes as the shorter but high intensity rainfall. A critical (threshold) rainfall volume was identified by Rahardjo et al (2007) for low permeable soils above which its effect on factor of safety is found to be insignificant

To investigate the impact of rainfall infiltration on low-permeable backfill soils, a few full scale/field tests were carried out [Stuglis 2010, Portelinha et al. (2013), Bui Van et al. (2017)]. Garcia et al. (2007), Yoo and Jang (2013), Melo et al (2021), Yoo et al. (2021) etc. used small-scale physical model testing to mimic rainfall infiltration characteristics with some of studies addressing the capillary barrier effect developed in unsaturated soil conditions [Junfeng et al. (2021, Portelinha et al. (2021)]. Centrifuge based physical model studies have been employed in a very limited number of works to study the effect of rainfall on retaining walls. Many studies including Tamate et al. (2012), Ling and Ling (2012),), Eab et al. (2014), Khan et al. (2018) etc. have developed rainfall simulators and infiltration models for testing at enhanced gravities in a centrifuge. The in-flight rainfall simulator used in the present study creates artificial rainfall as fine mist using specially designed pneumatic nozzles thereby facilitating the regulation of the intensity and duration of rainfall at high gravities.

Despite the relevance, very few centrifuge model studies have been conducted to assess the effect of varying rainfall pattern on the unsaturated properties of low-permeable soils. Hence, research on performance of geogrid reinforced soil walls with such low permeable backfills subjected rainfall conditions calls for more attention. In this study, two centrifuge tests are compared to ascertain the influence of rainfall intensity on the behaviour of a rigid facing geogrid reinforced wall with low permeable backfill soils.

2 CENTRIFUGE MODET TESTS

2.1 Model Materials used in the present study

Model soil used in the present study was formulated by blending locally available fine sand (SP as per USCS) and commercially available kaolin (CL as per USCS) in a ratio 4:1 (sand : kaolin) by dry weight. The model soil constituted of 80% sand, 10% silt and 10% clay with percentage of fines equal to 20%. The Liquid limit (LL), Plastic limit (PL) and Plasticity index (PI) of sand-kaolin mix are observed to be 11.86%, 9.78% and 2.08% respectively, on the basis of which the sand-kaolin blend represents a silty sand mixture, designated as SM as per USCS. The maximum dry unit weight (γ_{dmax}) and optimum moisture content (OMC) were determined as 18.75 kN/m^3 and 9% respectively by performing Standard Proctor compaction tests. In addition, the coefficient of permeability of the blended soil was observed to be 1.54 x 10^{-6} m/sec by conducting falling head test on moist-compacted soil samples placed at γ_{dmax} and OMC. The same soil was utilized for base layer as well as for the reinforced wall.

Following the scaling laws proposed by researchers like Viswanadham and König (2004), Viswanadham and Jessberger (2005) etc., a model geogrid (G1) was developed adhering to scaling criteria of tensile load strain characteristics and ensuring identical frictional bond behaviour and identical percentage open area between model and prototype geogrids. The model geogrid exhibited ultimate tensile loads of 0.873 kN/m and 0.959 kN/m and ultimate tensile strains of 45.81% and 25.15% in machine and cross machine directions respectively (ASTM D6637-15). A percentage open area (*f*) of 97.4% was ensured for both model and prototype geogrids to avoid loss of contact between soil-geogrid-soil and to prevent scale effects. The length of geogrid layers was oriented along the cross-machine direction. A model facing made of 10 mm thick (3 layers of 3 mm thick sheets joined using special wood glue) marine plywood sheet was used to replicate a prototype precast concrete panel wall facing of thickness of 185 mm. Facing element consists of six panels, connecting six layers of 200 mm long and 200 mm wide geogrid reinforcements adopted in centrifuge model with a vertical spacing (S_v) of 40 mm (model dimensions). The joint between the facing panels is in the form of Mortise and Tenon type.

2.2 Model Test Package and Instrumentation

The present study was carried out using a 4.5 m radius large beam geotechnical centrifuge facility available at the Indian Institute of Technology Bombay details of which were given by Chandrasekaran (2001). Fig. 1 shows the schematic cross section of model test package used in the present study. The internal dimensions of model container used are 760 mm in length, 200 mm in width and 410 mm in height. The front glass is made of Perspex glass whereas the other three walls are made of mild steel plate. Markers were glued to geogrid layers and facing panels and were tracked by four permanent markers. To simulate an initial ground water table, a seepage tank was placed on left side of the model container. Pore pressure transducers (PPTs) were placed at 25 mm (PPT4), 67.5 mm (PPT3), 187.5 mm (PPT2), and 240 mm (PPT1) from the seepage tank respectively, above the base layer of the model walls.

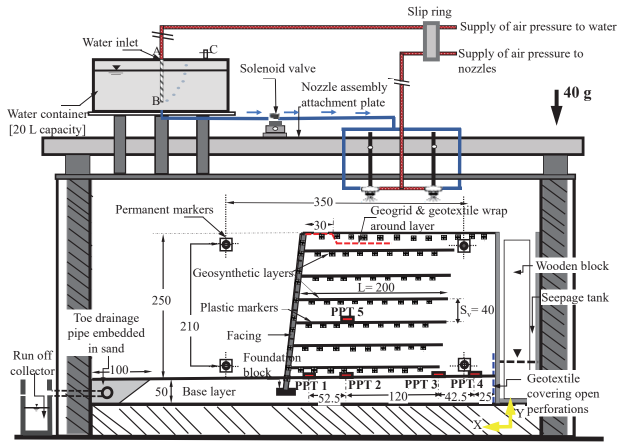

Fig. 1. Schematic cross section of model test package (dimensions in mm) [not drawn to scale]

The wall was constructed to a total height of 250 mm in seven soil layers, compacted at OMC and γd_{max}. Post the wall construction, a sand drainage layer was provided at the right side of the model container additionally with a toe drain comprising of a geotextile wrap-around pipe embedded into this sand drainage layer. In addition, the excess water flowing as run-off post soil saturation was collected in an acrylic container via a toe-drain pipe provided at the rear side of the mode strong box. The rainfall simulator was mounted on top of the model container which primarily consists of (1) a nozzle assembly attaching plate which is a slotted plate enabling horizontal shift of hanging rods attached with nozzles (2) a water container assembly which is an overhead tank [capacity= 20L] designed based on Modified Mariotte's principle, used for maintaining a constant water head during rainfall.

2.3 Test Programme

In the present study, two centrifuge model tests were conducted on reinforced soil walls by varying rainfall intensity but keeping wall dimensions, backfill material and geogrid reinforcement parameters constant. The wall height, H, was equal to 250 mm, simulating a wall of height 10 m in prototype dimensions at 40g. Wall face inclination (β) was equal to 84° with horizontal. Six layers of geogrid reinforcements were provided with a S_v

of 40 mm (S_v/H = 0.160). Model walls MW1 and MW2 were subjected to rainfall intensities of 10 mm/h and 20 mm/h respectively. Rainfall simulation in the centrifuge is based on pre-defined scaling laws wherein the rainfall intensity increases by N times in the centrifuge, while the rainfall duration reduces by $1/N^2$ times that of prototype rainfall events.

After mounting the entire test set up, the centrifuge was started, and the data acquisition system was logged on to record the voltage values received from the 4 PPTs. Post an equilibrating time of 15 minutes to establish the initial ground water table within the base layer, the water pressure and air pressure were set to the appropriate values to simulate the desired rainfall intensities. After 5 minutes, the solenoid valve was remotely activated, and the four nozzles positioned at 7 cm from the wall crest started to spray water in the form of fine mist. The rainfall was continued until wall failure occurred, or equilibrium conditions were achieved.

3 RESULTS AND DISCUSSION

The positive pore water pressures measured by the PPTs during the tests were recorded with the help of a data acquisition system at every one second interval, and images were captured in-flight at every 5 seconds interval by an on-board 12 Megapixel GoPro camera. Any movements experienced by the model walls with the progress of rainfall were determined by performing Digital Image Analysis (DIA) on pictures captured in-flight during centrifuge testing.

3.1 Pore water pressure and phreatic surface development during rainfall

The seepage behaviour of geogrid reinforced soil walls subjected to rainfall was investigated using pore water pressure readings obtained from pore pressure transducers (PPTs). The voltage values recorded by the PPTs were translated to corresponding pore water pressures (in kPa) by adopting proper calibration factors.

The phreatic surfaces within the model walls were then determined from the measured pore water pressures. Fig. 2 (a)-(b) present the phreatic surfaces developed during rainfall for the soil wall models Model MW1 and Model MW2 respectively, plotted at various time intervals till the onset of failure on the original wall profile. The head of water were obtained by converting the pore water pressures recorded into prototype values, and dividing them by the unit weight of water. Furthermore, photographs captured at the time of collapse are also included as insets into Fig. 2(a) – (b) indicating the failure condition and extent of deformations at the penultimate stage for both the models. Model MW1 registered continuously increasing positive pore water pressures with rainfall. Maximum pore water pressure developed at the time of failure was 62.2 kPa translating to a maximum total water head of 8.32 m measured at PPT 3. Meanwhile, in model MW2, it was observed that the model wall developed lesser positive pore water pressures even when subjected to a higher rainfall intensity of 20 mm/h. It achieved a maximum total water head of 6.69 m corresponding to a maximum pore water pressure of 46.2 kPa developed at the PPT3 position at the time of failure. In case of model MW2, the build-up of pore water pressure at the wall base was noted to be relatively slower after 9 days of rainfall with the growth in positive pore pressure less than 2% as observed in Fig. 2(b). This indicated that when a low-permeable backfill is subjected to a rainfall intensity much greater than its saturated hydraulic conductivity (k_s = 1.54 x 10^{-6} m/s), the infiltration rate reduces and majority of the water flows along the surface. This was substantiated by measuring the surplus water drained out and collected in the run- off collector during the centrifuge tests. It was ascertained that the collected discharge volume was higher (~ 4.5 litres) in the case of model MW2 subjected to a higher rainfall intensity of 20 mm/h even when the total rainfall duration was only half of that of model MW1 subjected to an intensity 10 mm/h (~2.18 litres).

3.2 Displacement vectors obtained in model soil

With the progress of rainfall, the wall models experienced movement in both the lateral and vertical directions. The displacements incurred by the L-shaped plastic markers were analysed in terms of the shift in their coordinates with reference to the global coordinates at salient time intervals with rainfall and represented as X_p and Y_p respectively on the abscissa and ordinate. Fig. 3(a)-(b) depict the displacement vectors plotted for Model MW1 and Model MW2 respectively on the basis of images taken at 40g before commencement of rainfall until the respective penultimate stage of centrifuge tests. Additionally, the normalized maximum face movement ($S_{f,max}$/H) and corresponding penultimate stage of each centrifuge test are also included in Fig. 3(a)-(b). The dashed lines represent the deformation profile of the model reinforced walls at the penultimate stage which is plotted using displacement incurred by the temporary markers along the facing and crest of the wall.

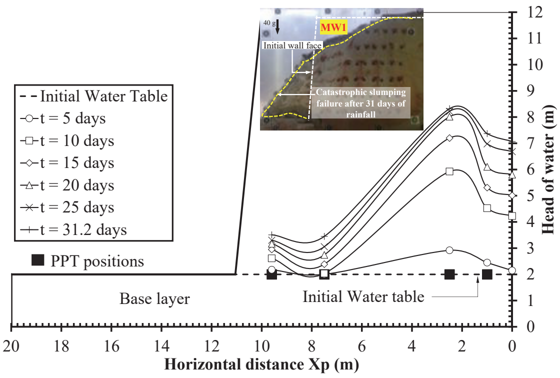

(a) Model MW1 [G1, n_g = 6; S_v = 1.6 m; I = 10 mm/h]

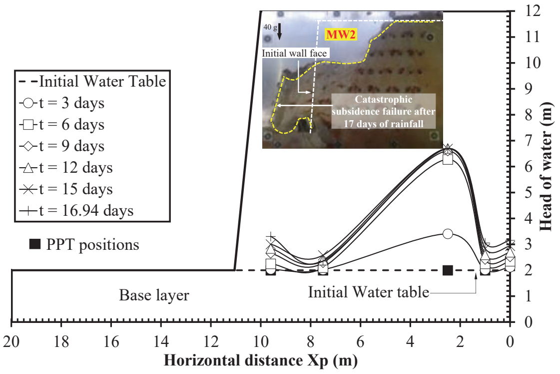

(b) Model MW2 [G1, n_g = 6; S_v = 1.6 m; I = 20 mm/h]

Fig. 2. Development of phreatic surfaces with rainfall within reinforced soil walls

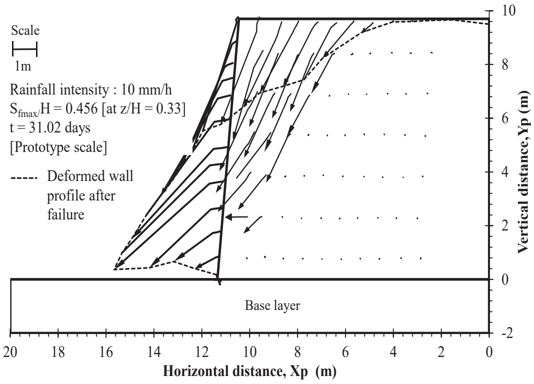

(a) Model MW1 [G1, n_g = 6; S_v = 1.6 m; I = 10 mm/h]

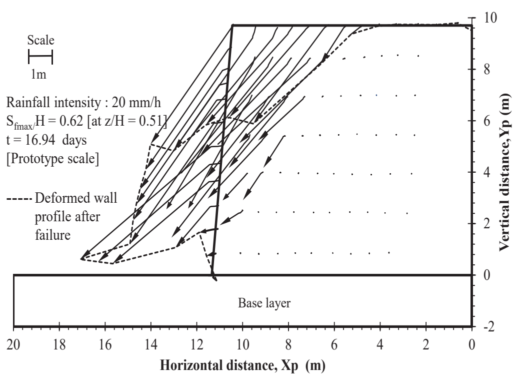

(b) Model MW2 [G1, n_g = 6; S_v = 1.6 m; I = 20 mm/h]

Fig. 3. Displacement vectors of reinforced soil walls subjected to rainfall

The displacement vectors for Model MW1 illustrated in Fig. 3 (a) clearly depicts that the weakest zone is inevitably the wall facing and crest region of the soil wall. The soil matric suction in reinforced zone started dropping with time as the wetting front descended gradually ultimately resulting in complete collapse of the wall within 27.5 mins [31.02 days in prototype dimension] of rainfall. In model MW2 as presented in Fig. 3 (b), the progression of surface settlements and face movements occurred faster, and the wall experienced a catastrophic failure in a shorter duration of 15.25 mins [16.94 days] with the application of 20 mm/h rainfall. In contrast to model MW1 where collapse was predominantly due to loss of suction, model MW2 underwent catastrophic slumping failure within a shorter period of time due to deformations generated by the significant volume of surface and subsurface flow. Moreover, the rainfall-induced settlements at the wall crest and face displacements for model walls MW1 and MW2 were deemed undesirable in terms of serviceability even before their final subsidence.

3.3 Strain distribution along the geosynthetic reinforcement layers

The strain contours for model wall MW1 and MW2 are depicted in Figs. 4(a)-(b) respectively at their penultimate stage of centrifuge tests clearly demarcating the distinct failure surfaces. The strain contour profile of Model MW1 indicates considerably higher straining due to complete global slip failure [Fig. 4(a)]. This resulted in rupture of geogrid layers in the upper section of the wall. All the geogrid layers exhibited strain less than ultimate tensile strain of G1 type geogrid [ε_{ug} = 25 %] till a period of 30 days of rainfall. However, at the penultimate stage [t= 31.02 days], the upper layers showed elevated strains.

The strain contours of Model MW2 [Fig. 4(b)] indicated that the magnitude of peak reinforcement strain encountered within the layers was almost comparable with model MW1. However, the geogrid straining in model MW2 accentuated due to the distress caused by higher rainfall intensity as the deteriorating effect of rainfall infiltration is accelerated when a higher rainfall intensity is applied.

4 CONCLUSIONS

Two centrifuge model tests were performed at 40 g on model geogrid reinforced soil walls of height 250 mm having 6° batter using a robust in-flight rainfall simulator. The model walls were subjected to rainfall intensities of 10 mm/h and 20 mm/h, and were compared to investigate the effect of varying rainfall pattern on the performance of the GRSW system. The following conclusions can be drawn from the test results:

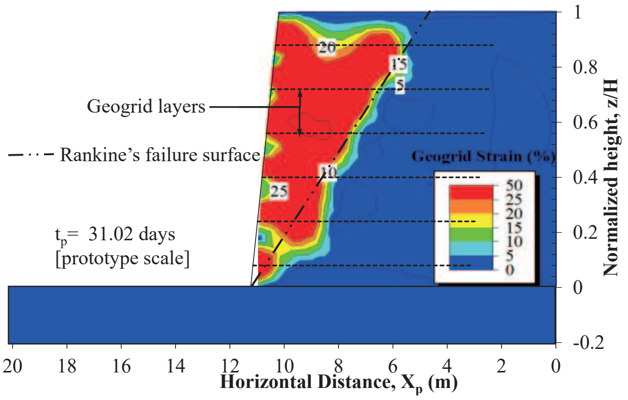

(a) Model MW1 [G1, n_g = 6; S_v = 1.6 m; I = 10 mm/h]

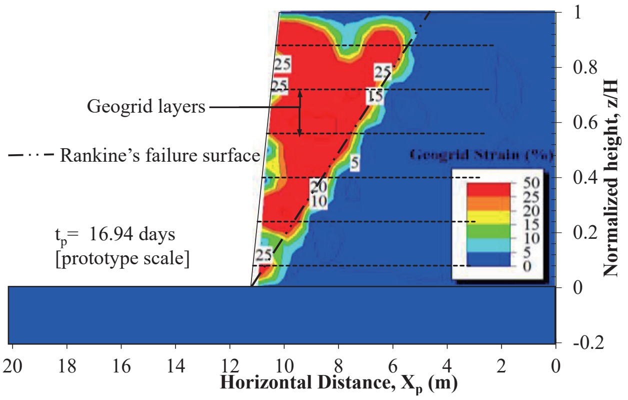

(b) Model MW2 [G1, n_g = 6; S_v = 1.6 m; I = 20 mm/h]

Fig. 4. Strain (in %) contours of centrifuge model walls at pen-ultimate stage

i. While the model wall subjected to rainfall intensity of 10 mm/h recorded failure after 31.02 days of rainfall, the wall subjected to higher rainfall intensity underwent a disastrous failure at a much earlier time [t = 16.94 days] but with comparable crest settlements and face movements. It can be stated that lower intensity longer duration rainfall caused similar wall displacements as high intensity short duration rainfall for the same amount of total precipitation.

ii. Lower values of pore water pressures were encountered in model wall subjected to 20 mm/h rainfall when compared to model wall subjected to a lower rainfall intensity of 10 mm/h. It implies that as the applied rainfall intensity exceeds the saturated hydraulic conductivity of the soil, the excess water translates into subsurface flow and walls fail mainly due to excessive wall deformations rather than loss of matric suction.

iii. The perpetual precipitation caused excessive straining in the geogrid layers subsequently resulting in rupturing of geogrid layers which resulted in the complete subsidence of the walls. However, when higher rainfall intensity was applied, the severe surface and subsurface flow deformations contributed to more distress in the geogrid layers, resulting in faster rupturing and early wall collapse.

The centrifuge results highlight the importance of drainage medium in geogrid wall sections constructed with low permeable backfill under rainfall conditions. Further studies are warranted to examine the effect of inclusion of a drainage element against rainwater infiltration, the location of initial water table and vertical spacing of geogrid layers within the wall cross-section. Also, it may be explored to further the study by measuring negative pore water pressures and soil moisture thereby facilitating the detection of descending wetting front during different stages of rainwater infiltration into the wall system.

ACKNOWLEDGEMENTS

The authors would like to acknowledge the staff and team members of the National Geotechnical Centrifuge Facility (NGCF) in IIT Bombay for their active cooperation and support throughout the present study.

REFERENCES

AASHTO. 2009. Standard specifications for highway bridges. *American Association of State Highway and Transportation Officials*, Washington. D.C. USA.

ASTM D6637. 2015. Standard test method for determining tensile properties of geogrids by the single or multi-rib tensile method. *American Society for Testing and Materials.*

Bhattacherjee, D. and Viswanadham, B.V.S. 2017, Design and Performance of an Inflight Rainfall Simulator in a Geotechnical Centrifuge. *American Society for Testing and Materials*. United States. 41(1): 72-91.

Bui Van, D., Chinkulkijniwat, A., Horpibulsuk, S., Yubonchit, S., Limrat, I., Arulrajah, A. and Jothityangkoon, C. 2017. Steady flow in mechanically stabilised earth walls using marginal soils with geocomposites. *Geosynth. Intl*. 24(6): 590-606.

Caicedo, B., Tristancho, J and Thorel, L. 2015. Mathematical and physical modelling of rainfall in centrifuge. *International Journal of Physical Modelling in Geotechnics*.15(3):150–164.

Chandrasekaran, V. 2001. Numerical and centrifuge modelling in soil structure interaction. *Indian Geotechnical J*. 31(1): 30–59.

Eab, K. H., Takahashi, A and Likitlersuang, S. 2014. Centrifuge modelling of root-reinforced soil slope subjected to rainfall infiltration. *Géotechnique* Letters. 4 (3):211-216.

Garcia, E. F., Gallage, C. P. K., and Uchimura, T. 2007, Function of permeable geosynthetics in unsaturated embankments subjected to rainfall infiltration, *Geosynth. Intl.* 14(2): 89-99.

Junfeng, T., Taro, U., Shangning, T., Dong, H., Jiren, X. 2021. Water movement and deformation in unsaturated multi-layered slope under heavy rainfall. *International Journal of GEOMATE, Geotechnique*, Construction Materials and Environment, Japan. 19(71): 174 – 181

Khan, I. U., Al-Fergani, M and Black. J. A. 2018. Development of a rainfall simulator for climate modelling. *Physical Modelling in Geotechnics*. – McNamara et al. (Eds) © 2018 Taylor & Francis Group, London, ISBN 978-1-138-34419-8: 501-512

Ling, H and Ling, H, I., 2012. Centrifuge Model Simulations of Rainfall-Induced Slope Instability", *J. Geotech. Geoenviron. Eng.,* ASCE. 138(9): 1151-1157.

Melo, M.T.S., Palmeira, E.M., Santos, E.C.G., da Luz, M.P. 2021. Geosynthetic performance against slope erosion caused by high intensity rainfall, *Geosynth. Int*. 28(4): 421–434.

Portelinha, F. H. M., Bueno, B.S., Zornberg, J.G. 2013. Performance of nonwoven geotextile-reinforced walls under wetting conditions: laboratory and field investigations, *Geosynth. Int*. 20(2): 90-104.

Portelinha, F. H. M., Santos, M.C., and Futai, M.M. 2021. A laboratory evaluation of reinforcement loads induced by rainfall infiltration in geosynthetic mechanically stabilized earth walls. *Geotextiles and Geomembranes.* 49: 1427–1439

Rahardjo, H., Rezaur, R.B and Leong, E. 2007.Factors Controlling Instability of Homogeneous Soil Slopes under Rainfall, *J. Geotech. Geoenviron. Eng.* ASCE. 133(12): 1532-1543.

Stuglis, R.P. 2010. Full scale MSE test walls. *In: Proc.,GRI-19 Conference*, Las Vegas. GII Publication, Folsom, PA, USA.

Tamate, S., Suemasa, N. and Katada, T. 2012. Simulation of precipitation on centrifugemodels of slopes. *International Journal of Physical Modelling in Geotechnics*. 12(3): 89–101.

Viswanadham, B. V. S and König, D. 2004. Studies on scaling and instrumentation of a Geogrid. *Geotext. Geomembr*. 22(5): 307-328.

Viswanadham, B.V.S and Jessberger, H. L. 2005. Centrifuge Modeling of Geosynthetic Reinforced Clay Liners of Landfills. *J. Geotech. Geoenviron. Eng*. ASCE. 131(5):564-574.

Xue, J. and Gavin, K. 2008. Effect of rainfall intensity on infiltration into partly saturated slopes. *Geotechnical and Geological Engineering*. 26(2): 199-209.

Yoo.C., Tabish, A., Yang, J.W., Abbas, Q. and Song, J.S. 2021. Effect of internal drainage on deformation behavior of GRS wall during rainfall. *Geosynthetics International*. https://doi.org/10.1680/jgein.21.00015